Runaway dynamics in disruptions with current relaxation events

István Pusztai[1], Mathias Hoppe[2], Oskar Vallhagen[1], and Tünde Fülöp[1]

[1] *Department of Physics, Chalmers University of Technology, Göteborg, SE-41296, Sweden*

[2] *Swiss Plasma Center, Ecole Polytechnique Fédérale de Lausanne, Lausanne, CH-1015, Switzerland*

During the thermal quench (TQ) of tokamak disruptions, chaotic field line regions form, causing a current profile relaxation, as well as elevated heat and particle transport. Using a mean-field helicity transport model [1] implemented in the disruption runaway modeling framework DREAM [2], we study the effects of current relaxation on the dynamics of runaway electrons (REs) [3]. Special attention is given to scenarios where flux surfaces remain intact in parts of the plasma. A skin current is induced at the boundary of the intact magnetic field region, that becomes an important center for the subsequent dynamics.

Simulation setup The DREAM simulations are performed in fully fluid mode, where the bulk electrons are characterized by their density n_e, temperature T_e and ohmic current density j_Ω, and the runaway electrons by the current density they carry j_{RE}. The Dreicer runaway generation rate is calculated using a neural network [4], Compton scattering and tritium decay seed sources are accounted for as in [5], the hot-tail seed is calculated using the model in [6, 7], and the avalanche growth rate accounts for partial screening [8]. The bulk electron temperature evolution is calculated from the time dependent energy balance throughout the simulation, according to Eq. (43) in [2], with additional heating by fluid runaway electrons, as (A.1) of [9].

The disruption simulations assume an initially ($t < 0$) ITER-like pure D-T plasma with a spatially constant electron density of $n_e = 10^{20}\,\mathrm{m}^{-3}$, and a parabolic electron temperature, T_e, with $20\,\mathrm{keV}$ on-axis, and a total plasma current of $I_p = 15\,\mathrm{MA}$. A realistically shaped plasma with major and a minor radius of $R_0 = 6\,\mathrm{m}$ and $a = 2\,\mathrm{m}$, and an on-axis magnetic field of $B_0 = 5.3\,\mathrm{T}$, is separated by $15\,\mathrm{cm}$ from a conducting wall with resistive wall time of $\tau_w = 0.5\,\mathrm{s}$.

At $t = 0$ additional neutral deuterium $7 \cdot 10^{20}\,\mathrm{m}^{-3}$ and neon $1.5 \cdot 10^{19}\,\mathrm{m}^{-3}$ is instantaneously and homogeneously deposited. At the same time an elevated transport of electron heat and energetic electrons is activated, along with a current profile relaxation. The corresponding diffusivities are calculated from a Rechester-Rosenbluth-type model [10], by taking appropriate moments of $D = \pi R_0 |v_\parallel| (\delta B/B)^2$, where the relative magnetic perturbation amplitude is set to $\delta B/B = 3.5 \cdot 10^{-3}$. At $t = 6\,\mathrm{ms}$, when the maximum plasma temperature has dropped to $\approx 100\,\mathrm{eV}$ the transport of energetic electrons and magnetic helicity is switched off, to account for the reformation of flux surfaces, and the electron heat diffusivity is reduced (technically

corresponding to $\delta B/B = 4 \cdot 10^{-4}$, while it may be caused by electrostatic turbulence then).

The current density relaxation is captured by evolving the poloidal flux ψ_p according to

$$\frac{\partial \psi_\mathrm{p}}{\partial t} = -\mathcal{R} + \mu_0 \frac{\partial}{\partial \psi_\mathrm{t}} \left(\psi_\mathrm{t} \Lambda_m \frac{\partial}{\partial \psi_\mathrm{t}} \frac{j_\mathrm{tot}}{B} \right), \tag{1}$$

where the toroidal flux $\psi_\mathrm{t}(r)$ is used as a radial coordinate. The term $\mathcal{R} = 2\pi \langle \mathbf{E} \cdot \mathbf{B} \rangle / \langle \mathbf{B} \cdot \nabla \varphi \rangle$, with the toroidal angle φ. This term describes ohmic dissipation, as $\langle \mathbf{E} \cdot \mathbf{B} \rangle = j_\Omega \langle B^2 \rangle / (\sigma B)$, with σ the electric conductivity, and j_Ω the ohmic current density. The total current density j_tot is related to the poloidal flux through Ampère's law, (49) in [2], and it includes the ohmic and the runaway current densities, j_Ω and $j_\mathrm{RE} \approx e c n_\mathrm{RE}$, with n_RE the RE density. The second term describes a local transport of magnetic helicity $H^\mathrm{M} = -2 \int \psi_\mathrm{p} \, d\psi_t$, with a transport coefficient Λ_m that we prescribe in space and time.

In the "intact core" scenario below, during the TQ we set a constant $\Lambda_m = 3 \cdot 10^{-2} \, \mathrm{Wb^2 m/s}$ for $r > 0.3 \, \mathrm{m}$, where the field is chaotic, and $\Lambda_m = 0$ below, where the flux surfaces remain intact, with a sharp but continuous transition in between. The RE transport is also disabled in the intact region. In the "intact edge" case the $r > 1.9 \, \mathrm{m}$ region is intact, with analogous settings.

Results First we consider the intact core case, the corresponding current density and temperature evolutions are shown in Fig. 1 on logarithmic contour plots. Panels a and c use the *low* remnant heat diffusivity quoted above. In the chaotic region, $r > 0.3$, j_tot flattens on a ms timescale, accompanied by the development of a skin current inside of the boundary of the intact region, that then diffuses resistively and broadens inward. At the end of the TQ, at $t \approx 6 \, \mathrm{ms}$, the temperature radiatively collapses almost everywhere in the plasma, except in a narrow region with high j_Ω. As the ohmic current decays in the rest of the plasma the induced electric field draws an increasing current here and it develops into a long-lived hot ohmic current channel. The peak temperature inside this channel is $> 200 \, \mathrm{eV}$, too high for radiation to dominate; it is radial heat transport out from this region than balances the ohmic heating. The heat transported to the colder edges of the current channel is then radiatively lost. The j_RE is very localized to the initial skin current region and it remains sub-dominant over the plotted time scale; it increases slowly and at later times eventually replaces the ohmic channel.

In the first $6 \, \mathrm{ms}$ the results shown in Figs. 1b and d are identical to those of a and c, but afterwards a higher remnant heat diffusivity is employed, at $\delta B/B = 2 \cdot 10^{-3}$. In this case the skin current layer diffuses away directly after the TQ, and it is replaced by a very strongly localized runaway beam, at the radius where the electric field in the skin layer reaches its highest value. Here the hot-tail source is many orders of magnitude higher than elsewhere, thus, even

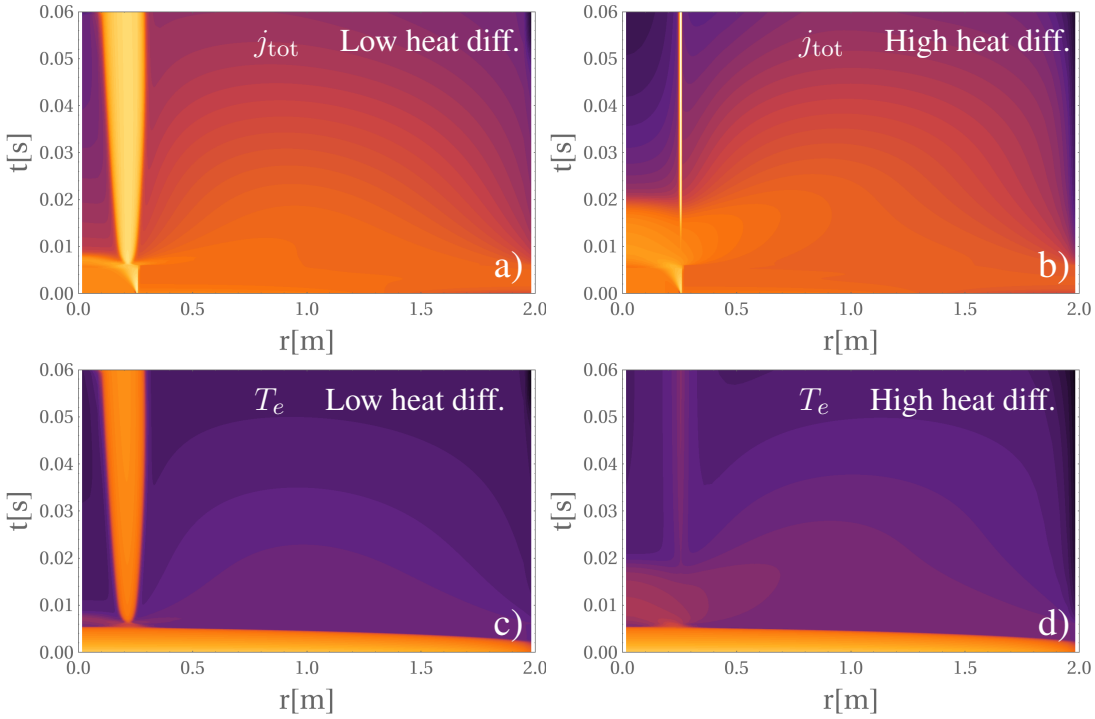

Figure 1: Logarithmic contour plots of the spatio-temporal evolution of the total current density (a-b) and the electron temperature (c-d), in case of an intact core, for low (a and c) and high (b and d) values of the remnant electron heat diffusivity.

though the final runaway current density is only logarithmically weakly dependent on the seed in strongly avalanching high-current devices, this is the only location where a significant runaway current is generated. Since it is inside the intact region it is not affected by a radial transport that could broaden the $j_{\rm RE}$ profile. Friction of the runaway beam on the bulk can only elevate the background temperature by a few eV in the vicinity of the current channel.

Next, we consider the intact edge scenario, where, similarly to the intact core, a sizable skin current develops, but now in the counter-I_p direction, seen in Figs. 2a. Due to the low edge temperature and the intact region being thin, the skin current diffuses away quite rapidly. Indeed at $t = 2\,\mathrm{ms}$, when the current relaxation of the inner, chaotic part of the plasma is not yet complete, the skin current has already started to decay. A small seed of counter-I_p runaway current is generated by the electric field in the skin layer. As this field is not sustained for a sufficiently long time, the runaway population remains insignificant. This does not need to be the case though; in some intact edge scenarios, significant reverse runway beams may be produced, as found in fully kinetic simulations in [3]. When the electric field changes sign in the skin region, the backward flowing energetic electrons can drift over to the forward direction without slowing down into the bulk, and provide a seed for forward runaway generation.

Finally we consider the effect of current relaxation on the I_p-spike. Without current relaxation

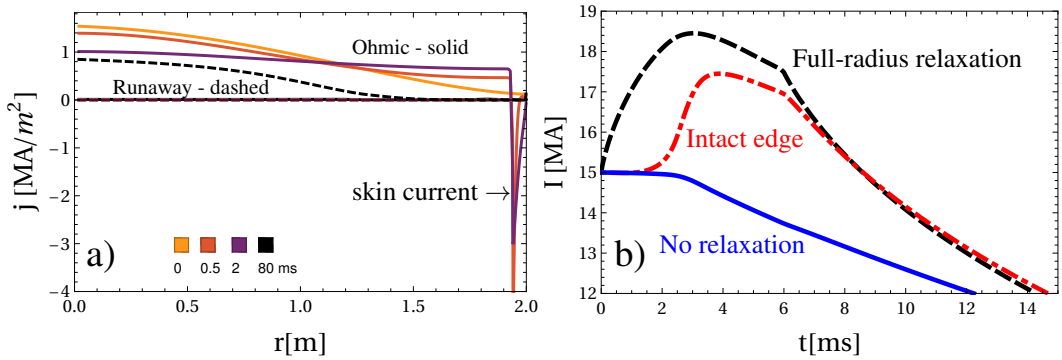

Figure 2: a: Current density profiles at different time steps, in case of an intact edge. b: Early evolution of the total plasma current in various current relaxation scenarios.

the total ohmic current decreases monotonically, as shown in Figs. 2b (solid line). When the current relaxation extends over the entire plasma, I_p starts to increase immediately as soon as Λ_m is activated (dashed). We note that in intact core scenarios the behavior is similar with somewhat lower I_p maximum. However, in the presence of an intact edge, the internal current relaxation remains temporarily invisible in the I_p signal, until the skin current layer resistively diffuses across the intact region. Thus the onset of the I_p spike is observed with a delay (dash-dotted) depending on the thickness and temperature of the intact region.

Conclusions In scenarios where flux surfaces remain intact in parts of the plasma, a skin current is induced at the boundary of the intact magnetic field region. This skin current region becomes an important center concerning the subsequent dynamics: It may turn into a hot ohmic current channel, or a sizable radially localized runaway beam, depending on the heat transport. If the intact region is in the plasma edge, runaway generation in the counter-current direction can occur, which may develop into a sizable reverse runaway beam. Revisiting such scenarios, accounting for the instability of current sheets, is a fruitful path for future studies. Even when the current relaxation extends to the entire plasma, the final runaway current density profile can be significantly affected, as the induced electric field is reduced in the core and increased in the edge, thereby shifting the center of runaway generation towards the edge.

[1] A H Boozer (2018) NF **58** 036006.
[2] M Hoppe et al (2021) CPC **268** 108098.
[3] I Pusztai et al (2022) subm. to JPP.
[4] L Hesslow et al (2019) JPP **85** 475850601.
[5] O Vallhagen et al (2020) JPP **86** 475860401.
[6] I Svenningsson (2020) MSc thesis, Chalmers.
[7] I Svenningsson et al (2021) PRL **127** 035001.
[8] L Hesslow et al (2019) NF **59** 084004.
[9] O Vallhagen et al (2022) NF accepted.
[10] A B Rechester et al (1978) PRL **40** 38.

This work was supported by the Swedish Research Council (Dnr. 2018-03911). This work has been carried out within the framework of the EUROfusion Consortium, funded by the European Union via the Euratom Research and Training Programme (Grant Agreement No 101052200 — EUROfusion). Views and opinions expressed are however those of the author(s) only and do not necessarily reflect those of the European Union or the European Commission. Neither the European Union nor the European Commission can be held responsible for them.